Journal of the Serbian Chemical Society
JSCS@tmf.bg.ac.rs • www.shd.org.rs/JSCS
J. Serb. Chem. Soc. *89* (9) 1227–1240 (2024)
JSCS–5783
Original scientific paper
Published 11 September 2024

Central composite design (CCD) and artificial neural network-based Levenberg–Marquardt algorithm (ANN–LMA) for the extraction of lanasyn black by cloud point extraction

AFAF AMARA-REKKAB[1,2]*

[1]*Institute of Science and Technology, Department of Hydraulics, University Center of Maghnia, Maghnia, Algeria and* [2]*Laboratory of Separation and Purification Technologies, Department of Chemistry - Faculty of Sciences, University of Tlemcen, Box 119, 13000, Algeria*

(Received 20 September, revised 8 November 2023, accepted 3 March 2024)

Abstract: The lanasyn black is among the most often used in manufacturing and is challenging to take out during the treatment of wastewaters from textile industry. The cloud point extraction was used for their elimination from an aqueous solution. The multivariable process parameters have been independently optimized using the central composite design and the Levenberg–Marquardt algorithm-based artificial neural network for the highest yield of the extraction of lanasyn black *via* the cloud point extraction. The CCD forecasts the output maximum of 97.01 % under slightly altered process parameters. Still, the ANN–LMA model predicts the extraction yield (99.98 %) using 1.04 g of KNO_3, the beginning pH of solution 8.99, the initial content of lanasyn black 24.57 ppm and 0.34 mass % of Triton X-100. With the coefficients of determination of 0.997 and 0.9777, the most recent empirical verification of the model mentioned above predictions using CCD and ANN–LMA is determined to be satisfactory.

Keywords: dyes; wastewater; extraction; optimisation; surface methodology; neural models; environment.

INTRODUCTION

The pollutant levels in wastewater from textile manufacturers are typically high. They include up to 1 g/L of the particles and significant levels of organic contaminants in soluble and colloidal forms. In any case, their colour intensity as a function of dilution is one of the most distinctive indicators of textile industry effluent pollution.[1–4] The colour of wastewater can be mostly attributed to the

* E-mail: amarafaf@yahoo.fr
Dedicated to the memory of Professor Mohamed Amine DIDI, who passed away on January 17, 2023. You will never be forgotten, my dear Professor.
https://doi.org/10.2298/JSC230920022A

Available online at: http://www.shd.org.rs/JSCS

(CC) 2024 Serbian Chemical Society.

widespread use of organic dyes in the textile industry. During the manufacturing, dyes are applied to fibres, textiles and final goods, depending on the business' expertise. Between 10 and 50 % of the pigments used throughout the dying procedure are still present in the technical waste solutions and cleaning water that is produced after cleaning the dyed articles.[5] Because of this, the intensity of colour in wastewaters from textile businesses that use dyes during the production cycle might approach 1:1000. The amount of colouring and the level of dilution in the home and industrial wastewater discharged simultaneously. Using green and sustainable technology necessitates the application of alternative processes that utilise fewer organic solvents.[7]

Until now, numerous methods for removing dyes from aqueous solutions, industrial detritus and polluted water have been reported, including the following: adsorption, electrochemical process, flocculation, membrane filtration, chemical oxidation and biodegradation.[8–10]

Over the past ten years, the cloud point extraction (CPE) is an effective extraction method and has continuously developed.[11,12] CPE has several advantages over conventional pre-treatment methods, including the ease of use, increased efficiency, safety and environmental friendliness.[13] To obtain phase separation from the extraction solution, the solubilisation of the surfactant and cloud point phenomena are used primarily.[14] Typically, the hydrophilic phase of a surfactant expands in water to produce a long, flexible vermiform micelle. As a result, a tiny volume of the surfactant-rich phase might contain a large amount of the analytes that interact with micellar systems. The analytes move to the inside of the micelles and become securely attached to the hydrophobic groups once the concentration of the surfactant exceeds the micelles' critical point, and therefore micelles will form.[15,16] Contrary to the most traditional non-ionic surfactants, Triton X-100 (T100) is a non-ionic surfactant with a distinct structure of the hydrophobic component T100, specifically, features an alkyl-aryl (octyl-phenyl) group as its hydrophobic component instead of an aliphatic tail. It is widely employed in the field of biochemical research as well as in some pharmaceutical formulations and biological system applications.[17]

Clariant of Switzerland manufactures the anionic azo dye lanasyn black M--DL, also known as lanasyn black. The dye is one of the most frequently used in manufacturing and is difficult to eliminate during the effluent treatment.[5]

Our work's objective focuses on removing lanasyn black by the cloud point extraction using the non-ionic extractant T100 and the ionic liquid Aliquat 336. A salting-out technique was implemented, which permits the phase separation of surfactants with high cloud points, including T100, at room temperature. When combining a nonionic salt with an inorganic salt (KNO_3), the cloud point of a surfactant solution decreases as the salt concentration increases. The reason for this is because the water molecules surrounding the nonionic surfactant exhibit a

(CC) 2024 Serbian Chemical Society.

higher degree of the orientation towards the salt anions (such as NO_3^-) even under normal room temperature conditions.[18] The influence of function variables was studied using a central composite design and artificial neural network based on Levenberg–Marquardt algorithm. The optimal conditions of the extraction of our dye were determined.

MATERIAL AND METHODS

Materials

T Complex Textile (Soitex) in Tlemcen, Algeria, sells black lanasyn ($C_{38}H_{32}CrN_8O_{10}S_2$). Triton X-100 is a non-ionic surfactant with an HLB value of 13.5 and a critical micelle concentration (*CMC*) of 3.0×10^{-4} M at 25 °C, was employed in this investigation. KNO_3 99 % came from Merck, used to decrease the point cloud temperature to room temperature. Aldrich is the source of Aliquat 336 (tri-capryl-methyl-ammonium chloride, $CH_3N[(CH_2)_7CH_3]_3Cl$). Sigma–Aldrich manufactures sodium hydroxide and hydrochloric acid. Chemopharma provides the ethanol 96 % needed. To make our solutions, we used distilled water.

Batch extraction experiments

Every alteration done throughout this work is based on the Triton X-100 and added mass of KNO_3 cloud point extraction of the organic contaminant black lanasyn (LN). At room temperature and in graduated tubes, from 1.5–4 % of Triton X-100 was added to Na_2SO_4 from 0.5–1 g, added to 1mL of Aliquat 336 at 0.3 M dissolved in 5 mL of the mother solution of LN from 10 to 20 ppm and then supplemented up to 10 mL with the same solution. The solution's pH ranged from 2.4–6.82. The solutions are left to stand for 30 min. Then, they were centrifuged at 2000 rpm for 10 min, and UV–Vis measures the diluted phase at the absorption band λ_{max} = 570 nm. The various procedures taken throughout LN organic pollutant extraction using cloud point are shown in Fig. 1.

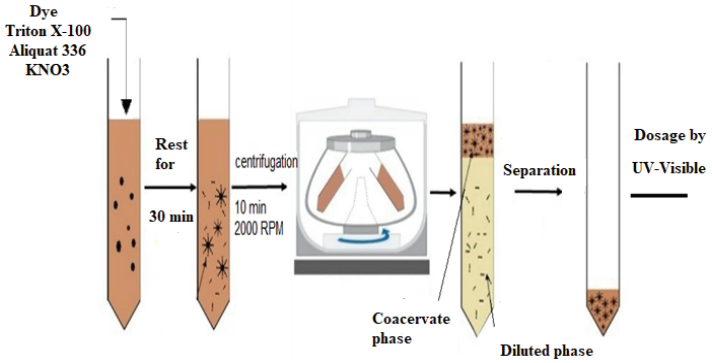

Fig. 1. Schema of the CPE of lanasyn black.

The black lanasyn solutions' UV–Vis absorbance was measured using an SP-UV 200S UV–Vis spectrophotometer. Adwa pH-metre was used to measure pH. The LN removal efficacy (%) was calculated by:[19,20]

$$\text{Removal}(\%) = 100\frac{C_i - C_e}{C_i} \quad (1)$$

(CC) 2024 Serbian Chemical Society.

where C_i is the initial concentration and C_e is the equilibrium concentration of LN.

Central composite design

The central composite design (CCD) is the most frequently employed among all multivariate methods. CCD determines how each component affects how the other factors interact. With the least amount of time and effort, this method establishes the system's ideal circumstances. This approach focuses on achieving several specific objectives, the most crucial of which is to enhance the process by identifying the best input.[21]

In this work, CCD was successfully employed to examine the impact of various variables on the effectiveness of lanasyn black's extraction by the cloud point extraction. Four distinct factors' experimental ranges and levels were selected. Table I lists the mass of KNO_3 (X_1), Triton X-100 (X_2), initial pH of the solution (X_3) and initial dye concentration (X_4). The following equation was used to calculate the results of 31 experimental runs. The following Equation was used to code the factors:[22–24]

$$x_i = \frac{X_i - X_0}{\Delta X} \tag{2}$$

where x_i, X_i, X_0, and ΔX are the coded values of the factors, their corresponding real values, the centre point of the real independent variable and the step between the real variables, respectively.

The multi-regression polynomial equation (Eq. (3)) can be used to represent the mathematical representation of relating the independent factor to the outcome:[25–27]

$$y(\%) = A_0 + \sum_{i=1}^{k} A_i X_i + \sum_{i=1}^{k} A_{ii} X_i^2 + \sum_{i=1} \sum_{j=i+1} A_{ij} X_i X_j + \varepsilon \tag{3}$$

As far as they are concerned, A_0 denotes the expected response, A_i, A_{ii}, A_{ij} represents the constant coefficient, and X_i, X_j represents the input components in coded values. Finally, it means the overall error. Statistical software Design Expert 13 created the response surface, contour plots and statistical data analysis.

TABLE I. Summary of CCD design

Level	Experimental factors with their units			
	Mass of KNO_3 (X_1)	Triton X-100 (X_2)	pH of the solution(X_3)	Initial dye concentration (X_4)
–2	0.25	0.025	0.19	5
–1	0.5	0.15	2.4	10
0	0.75	0.275	4.61	15
1	1	0.4	6.82	20
2	1.25	0.525	9.03	25

Artificial neural network–Levenberg–Marquardt algorithm (ANN–LMA)

The artificial neural network simulation is a mathematical instrument. It predicts the linear and nonlinear relationships between multiple inputs and outputs in a complex process. Individually, ANN and CCD can be used to optimise the non-linear process parameters of our dye extraction; however, they are highly interdependent on the input parameters. Due to the presence of beams of highly corresponding elements known as neurons, ANN is regarded as more accurate than CCD.[28–30] Input, hidden and output layers are the distinct divisions of multiple neurons that comprise the ANN model. Hidden layers, which can have a single or mul-

(CC) 2024 Serbian Chemical Society.

tiple architectures, are the operating units that function as the character detectors and introduce nonlinearity into the network. The development of an ANN model is contingent upon multiple phases.[31–33] The phase of learning and the phase of validation. Using previously presented CCD data and the Levenberg–Marquardt feedback algorithm, an ANN model was developed and trained. However, the data points were generated using the second-order polynomial equation of CCD. Fig. 2 shows the simple structure of the current ANN–LMA.

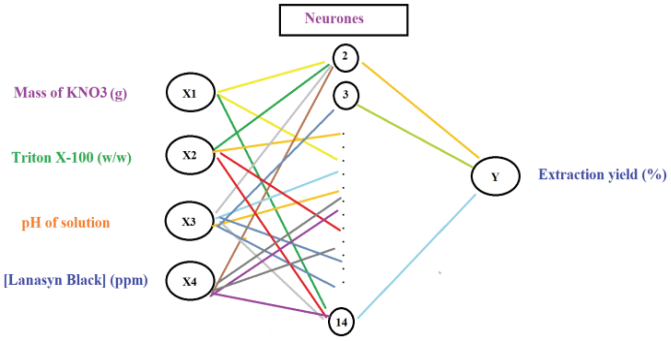

Fig. 2. Proposed modelling by ANN–LMA.

As the error functions, we used the mean absolute error (*MAE*), the mean square error (*MSE*), the root mean squared error (*RMSE*) and the absolute average deviation (*AAD*) to evaluate the performance of the ANN model for predicting the dependent variable. It is determined using the following equations:[28]

$$MAE = \left(\frac{1}{n}\right)\sum_{i=1}^{n}\left|E_{\text{model}} - E_{\text{exp}}\right| \tag{4}$$

$$MSE = \frac{\sum_{i=1}^{n}\left(E_{\text{model}} - E_{\text{exp}}\right)^2}{n} \tag{5}$$

$$ADD(\%) = \frac{100}{\text{n}}\left(\sum_{i=1}^{n}\frac{\left|E_{\text{model}} - E_{\text{exp}}\right|}{E_{\text{exp}}}\right) \tag{6}$$

$$RMSE = \sqrt{\frac{\sum_{i=1}^{n}\left(E_{\text{model}} - E_{\text{exp}}\right)^2}{n}} \tag{7}$$

RESULTS AND DISCUSSION

Statistical results

According to the combinations selected using central composite modelling, the experimental matrix shown in Table II comprises 31 experiments. Using this approach, we identified the four elements that were evaluated that were the most critical parameters and the synergic interactions.

The five-level matrix generated by CCD and ANN–LMA with the responses obtained experimentally for the extraction of our dye is shown in Table II. It is

(CC) 2024 Serbian Chemical Society.

clear from the Table II that the extraction yield was obtained around the centre of all parameters. The anion of lanasyn black, negatively charged, reacts in the coacervate phase, Triton X-100 and the ammonium cation of Aliquat 336 form mixed micelles as shown in Fig. 3.[34]

TABLE II. Experimental matrix of experimental data, CCD and ANN–LMA for the extraction of lanasyn black

Run order	Mass of KNO_3 (%)	Triton X-100 (mass %)	pH	Lanasyn black (ppm)	Extraction yield (%)	Predicted value by CCD (%)	Predicted value by ANN (%)
1	–1	–1	–1	–1	88.98	86.6054	88.8945302
2	–1	1	1	–1	90.22	89.2438	90.2931885
3	1	1	–1	1	83.24	84.2225	84.1005084
4	1	1	–1	–1	91.00	89.8971	91.2489692
5	1	–1	1	1	83.60	84.1642	84.4159927
6	1	–1	–1	–1	89.83	92.3075	90.6289325
7	1	–1	1	–1	82.44	81.9387	83.89133
8	0	0	0	0	96.78	97.5114	97.7391311
9	2	0	0	0	88.26	86.6404	89.4786037
10	0	0	0	0	98.02	97.5114	97.7391311
11	–1	–1	1	–1	82.59	82.7492	83.2669267
12	–1	1	–1	–1	84.66	85.2375	83.0878711
13	–1	–1	–1	1	82.30	84.0508	84.4210992
14	0	0	2	0	93.15	93.7221	93.9104141
15	1	–1	–1	1	84.91	85.1054	86.2595135
16	–2	0	0	0	86.18	87.4388	87.6001534
17	0	0	0	0	98.00	97.5114	97.7391311
18	0	0	–2	0	91.59	90.6571	91.4822843
19	0	0	0	0	97.00	97.5114	97.7391311
20	0	2	0	0	82.74	83.4954	83.0456114
21	–1	1	–1	1	84.49	84.2104	84.5912063
22	0	0	0	2	91.28	89.5638	91.6904094
23	–1	–1	1	1	89.30	89.6221	88.7290656
24	1	1	1	1	89.55	91.1438	91.1766252
25	0	0	0	0	98.02	97.5114	97.7391311
26	–1	1	1	1	98.98	97.6442	98.3143374
27	0	–2	0	0	79.00	77.8838	79.963546
28	1	1	1	–1	88.00	87.3908	90.3381571
29	0	0	0	0	97.76	97.5114	97.7391311
30	0	0	0	0	97.00	97.5114	97.7391311
31	0	0	0	–2	87.01	88.3654	89.8871532

On the basis of these findings, the empirical relationships between the response of CCD and selected variables have been determined:

$$\text{Extraction yield (\%)} = 97.511 - 0.200m(KNO_3) + 1.403\times\text{Triton X-100} + \\ + 0.766\text{pH} + 0.300[\text{LN}] - 2.618m(KNO_3)m(KNO_3) - 4.205\times\text{Triton}$$

(CC) 2024 Serbian Chemical Society.

$$X\text{-}100\times\text{Triton X-}100 - 1.330\text{pH}\times\text{pH} - 2.137[\text{LN}][\text{LN}] - 0.261m(KNO_3)\times$$
$$\times\text{Triton X-}100 - 1.628m(KNO_3)\text{pH} - 1.162m(KNO_3)[\text{LN}] + 1.966\times$$
$$\times\text{Triton X-}100\times\text{pH} + 0.382m(\text{Triton X-}100)\times[\text{LN}] + 2.357\text{pH}[\text{LN}]$$

To find the significant main and interaction effects of the dye extraction parameters, an ANOVA (Table III) was performed.

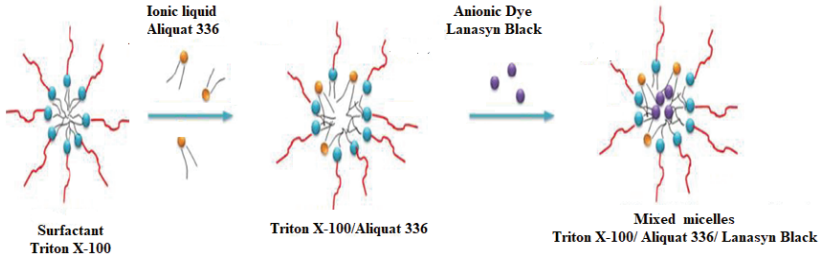

Fig. 3. Lanasyn black dye extraction using combined Triton X-100/Aliquat 336 micelles.

TABLE III. ANOVA for CCD-quadratic model

Source	Sum of squares	*df*	Mean square	*F*-value	*p*-value	Significance
Model	706.27	14	50.45	16.50	< 0.0001	Significant
A-Mass of KNO_3	0.9560	1	0.9560	0.3128	0.5863	
B-Triton X-100	47.24	1	47.24	15.45	0.0020	
C-pH	14.09	1	14.09	4.61	0.0529	
D-[Lanasyn black]	2.15	1	2.15	0.7047	0.4176	
AB	1.09	1	1.09	0.3555	0.5621	
AC	42.41	1	42.41	13.88	0.0029	
AD	21.60	1	21.60	7.07	0.0209	
BC	61.82	1	61.82	20.22	0.0007	
BD	2.33	1	2.33	0.7633	0.3994	
CD	88.88	1	88.88	29.08	0.0002	
A^2	146.45	1	146.45	47.91	< 0.0001	
B^2	377.68	1	377.68	123.56	< 0.0001	
C^2	37.88	1	37.88	12.39	0.0042	
D^2	97.59	1	97.59	31.93	0.0001	
Residual	36.68	12	3.06			
Lack of fit	35.83	10	3.58	8.38	0.1113	Not significant
Pure Error	0.8552	2	0.4276			
Cor total	742.95	26				
Model			$Adeq_{Precision}$ 15.1637	R^2 95.06 %	$R^2_{(adjust)}$ 89.30 %	$R^2_{(predicted)}$ 71.97 %

The model *F*-value of 16.50 to $F_{critic}(0.05, 14.12) = 2.65$ indicates that the model is statistically significant. There is only a 0.01 % possibility that this large cloud's *F*-value is caused by noise. *p*-Values less than 0.05 indicate the significant model terms. In this particular instance, Triton X-100, mass of KNO_3×pH,

(CC) 2024 Serbian Chemical Society.

mass of KNO_3×[Lanasyn black], Triton X-100×pH, pH×[Lanasyn black], (mass of KNO_3)^2, (Triton X-100)^2, pH^2 and [Lanasyn Black]^2 are significant model terms. The values exceeding 0.1000 indicate that the model terms are not statistically significant. The lack of fit *F*-value of 8.38 indicates that the lack of fit is not statistically significant in comparison to the pure error (0.05, 10.2) = 19.4. Due to noise, there is an 11.13 % probability that a lack of fit *F*-value will occur in this large cloud. The predicted R^2 of 0.7197 corresponds reasonably well to the adjusted R^2 of 0.8930, *i.e.*, the difference is less than 0.2. $Adeq_{Precision}$ measures the signal-to-noise ratio. The obtained ratio of 15.164 indicates a sufficient signal. This model can be used to navigate the design space.

Contour plots and response surfaces

Fig. 4 is a graphical representation of the correlations between significant, optimal values and the specific output variability by the contour plots and response surface. By the possible point extraction, these images aid in understanding and describing the combined impact of the two variables on lanasyn black extraction.[35] Depending on the contour plot's morphologies, the interaction's significance may be high if the contour plot is elliptical and saddle-shaped, but low if it depicts a circular shape. The maximum response value under the influence of the operational inputs was effectively determined by keeping the remaining pair of factors at their midpoint at the same time.[36]

The elliptical contour diagrams depict the significant impact of interactions between the mass of KNO_3×pH, mass of KNO_3×[Lanasyn black], Triton X--100×pH, and pH×[Lanasyn black]. The maximum extraction yield was achieved at the centre level of all parameters, suggesting significance.

Response optimization

The response optimization was used to optimize the extraction in MINITAB 19.0, and the experiment was run at the specified solution, yielding an extraction rate of 97.87 %, which was extremely close to the predicted value. The mass of KNO_3 was 1.07575 g, Triton X-100 was 0.368 mass %, the beginning pH of the solution was 9.03, the initial concentration of black lanasyn was 22.575 ppm, and this combination produced the highest extraction yield.

ANN–LMA modelling

Using a feed-forward back propagation network and the Levenberg–Marquardt algorithm, the ANN-GA model was developed. Three data set subdivisions were generated. Each subset contained 80 % of the testing data, 10 % of the validation data, and 10 % of the network training data. It is important to note that these divisions were wholly arbitrary. The inputs and outputs are immutable elements of the ANN's topology (architecture). Moreover, the number of concealed layers and their respective neurons represent a series of variable elements.

(CC) 2024 Serbian Chemical Society.

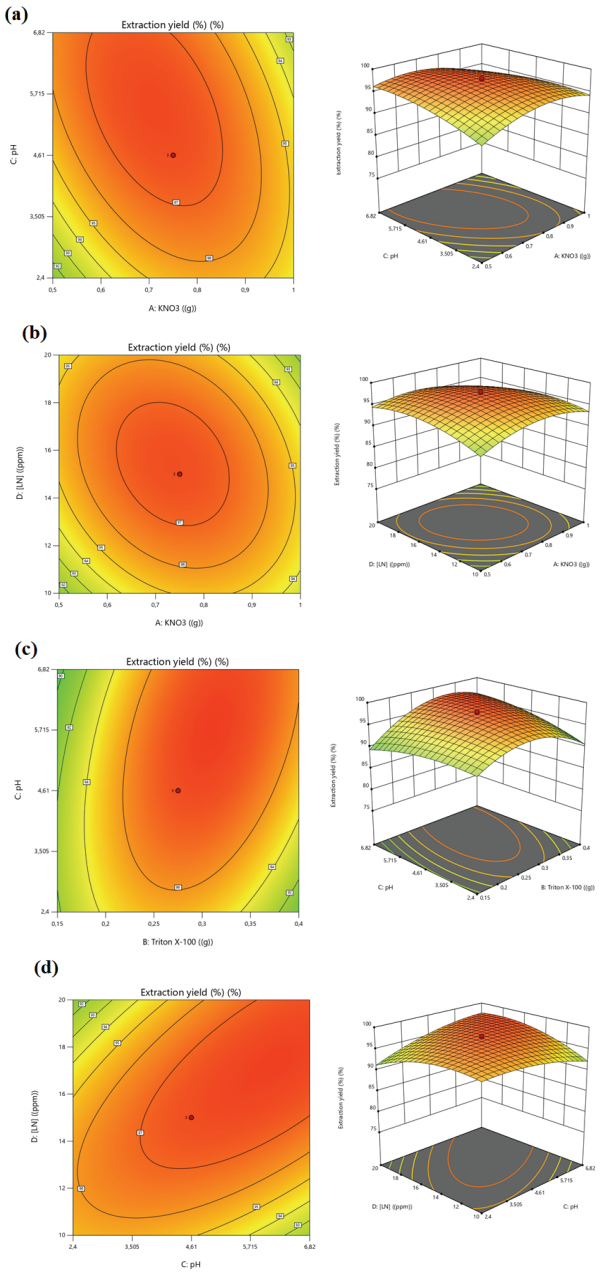

Fig. 4. Contour plots and response surface of the effects: a) mass of KNO_3 and initial pH of the solution; b) mass of KNO_3 and initial concentration of Lanasyn black; c) Triton X-100 and initial pH of the solution; d) initial pH of the solution and initial concentration of lanasyn black on the extraction of lanasyn black by cloud point extraction.

(CC) 2024 Serbian Chemical Society.

Fig. 5 shows that the learning converged after 9 periods with the lowest average square error. Thus, during the ANN iterative learning, the model achieved a maximum R-value of 0.987772 (Fig. 6a) and a minimum MSE value of 2.0727×10^{-3} (Fig. 6b) at nine epochs for ten neurons in the hidden layer. Therefore, the best 4–10–1 network architecture is used for the process optimization, representing 4 entries in the first layer, 10 hidden neurons, and one upper layer output. The R^2 value close to 1 and a low MSE value indicate that the performance of the developed model is satisfactory and corresponds to the experimental extraction values of the LN per point of disruption.

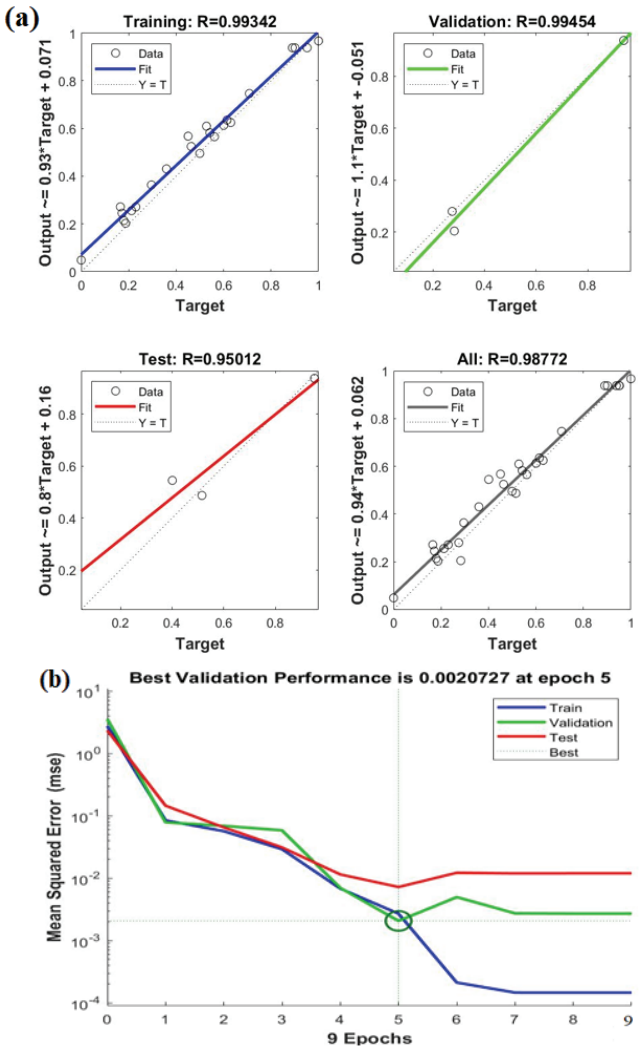

Fig. 5. Regression and performance plots of the ANN–LMA model.

(CC) 2024 Serbian Chemical Society.

The reliability of the here given model for predicting the maximum output data was confirmed while using the optimal points suggesting the ANN37 (KNO_3 mass: 1.04 g; beginning pH of solution 8.99, initial of Black Lanasyn 24.57 ppm, and 0.34 mass% of Triton X-100). The extraction yield of the experimentally recorded LN was 99.98 % suggesting the suitability and validity of the model. However, the optimums achieved by ANN resulted in an even higher extraction yield than with CCD modelling.[38–41]

Comparative study between CCD and ANN–LMA

In order to evaluate the efficacy of the CCD and ANN models, the outputs were compared to the relevant experimental data, Fig. 6.

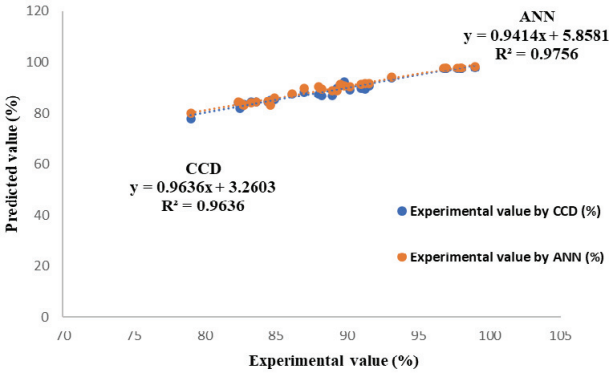

Fig. 6. Comparative parity diagram of experimental and predicted results.

The determination coefficient R = 0.97498 for the CCD model and R = = 0.98772 for the ANN model shows that the values of the model-based predictions are in perfect accordance with the experimental results.

As a result, the proposed models are well-adapted to data and provide stable responses. However, compared to the RSM model, the ANN model has a higher predictive capacity and accuracy based on the experimental results. The R value is closer to 1.0.

In addition to the regression coefficient (R), the observed *MAE*, *MSE*, *AAD*, and *RMSE* values for both models were determined to provide a statistical indication of the accuracy of the model predictions. The *MAE*, *MSE*, *AAD* and *RMSE* values for the CCD and ANN models have been calculated and are presented below.

The *MAE* (0.1203), *MSE* (0.4488), *AAD* (0.1363 %) and *RSME* (0.6699) for the CCD model are higher than those (0.0955, 0.2831, 0.1097 and 0.5321 %, respectively) for the ANN model. This means the ANN model offers a higher modelling capacity than the CCD model. This result is similar to several researchers.[42,43]

(CC) 2024 Serbian Chemical Society.

CONCLUSION

The lanasyn black was obtained by the textile sector, and is among of the more frequently used in manufacturing. It is difficult to remove during wastewater treatment. Their removal in an aqueous solution was accomplished by the cloud point extraction. For the most significant yield of the extraction of lanasyn black using the cloud point extraction, the multivariable process parameters have been independently optimized using the central composite design (CCD) and artificial neural network–Levenberg–Marquardt algorithm (ANN–LMA). The ANN–LMA model predicts the extraction yield (99.98 %) in the optimal conditions. The most recent experimental validation of the model mentioned above predictions using ANN–LMA and CCD is found to be good, with coefficients of determination of 0.997 and 0.9777, respectively.

ИЗВОД

ЦЕНТРАЛНИ КОМПОЗИТНИ ДИЗАЈН (CCD) И LEVENBERG–MARQUARDT АЛГОРИТАМ ЗАСНОВАН НА ВЕШТАЧКОЈ НЕУРОНСКОЈ МРЕЖИ (ANN–LMA) ЗА ИЗДВАЈАЊЕ ЛАНАСИН ЦРНЕ БОЈЕ ЕКСТРАКЦИЈОМ У ТАЧКИ ЗАМУЋЕЊА

AFAF AMARA-REKKAB[1,2]

[1]Institute of Science and Technology, Department of Hydraulics, University Center of Maghnia, Maghnia, Algeria и [2]Laboratory of Separation and Purification Technologies, Department of Chemistry – Faculty of Sciences, University of Tlemcen, Box 119, 13000, Algeria

Ланасин црна боја је међу најчешће коришћеним у производњи, нарочито текстилној индустрији, и тешко је уклонити је током третмана отпадних вода. За њену елиминацију у воденом раствору коришћена је екстракција у тачки замућења. Параметри мултиваријантног процеса су независно оптимизовани коришћењем централног композитног дизајна и вештачке неуронске мреже, засноване на Levenberg–Marquardt алгоритму за највећи принос екстракције Ланасин црне боје у тачки замућења. CCD предвиђа излазни максимум од 97,01 %, под благо измењеним параметрима процеса. Ипак, ANN–LMA модел предвиђа принос екстракције од 99,98 %, користећи количину KNO_3 од 1,04 g, почетни pH раствора 8,99, почетну вредност ланасин црне боје од 24,57 ppm и 0,34 мас. % Тритона X-100. Са коефицијентима детерминације од 0,997 и 0,9777, одређена је задовољавајућа најновија емпиријска верификација предвиђања модела помоћу CCD и ANN–LMA.

(Примљено 20. септембра, ревидирано 8. новембра 2023, прихваћено 4. марта 2024)

REFERENCES

1. D. A. Yaseen, M. Scholz, *Int. J. Environ. Sci. Technol.* **16** (2019) 1193 (https://doi.org/10.1007/s13762-018-2130-z)
2. B. K. Nandi, A. Goswami, M. K. Purkait, *Appl. Clay. Sci.* **42** (2009) 583 (https://doi.org/10.1016/j.clay.2008.03.015)
3. I. G. Krasnoborodko, *Destructive wastewater treatment from dyes*, L: Chemistry, 1988
4. M. Ghaedi, H. Hossainian, M. Montazerozohori, A. Shokrollahi, F. Shojaipour, M. Soylak, M. K. Purkait, *Desalination* **281** (2011) 226 (https://doi.org/10.1016/j.desal.2011.07.068)

(CC) 2024 Serbian Chemical Society.

5. V. Geissen, H. Mol, E. Klumpp, G. Umlauf, M. Nadal, M. D. Ploeg, S. E. A. T. M. van de Zee, C. J. Ritsema, *Int. Soil Water Conserv. Res.* **3** (2015) 57 (https://doi.org/10.1016/j.iswcr.2015.03.002)
6. N. E.Djebbari, A. Amara, A. Didi, M. A. Didi, *Sci. Study Res. Chem. Chem. Eng., Biotech., Food Ind.* **23** (2022) 333 (https://pubs.ub.ro/dwnl.php?id=CSCC6202204V04S01A0005)
7. H. Chandarana, P. Senthil Kumar, M. Srinivasan, M. Anil Kumar, *Chemosphere* **285** (2021) 131480 (https://doi.org/10.1016/j.chemosphere.2021.131480)
8. M. K. Dahri, M. R. R. Kooh, L. B.L. Lim, *Alex. Eng. J.* **54** (2015) 1253 (https://doi.org/10.1016/j.aej.2015.07.005)
9. E. Brillas, E.Mur, R. Sauleda, L. Sanchez, J. Peral, X. Domenech, J. Casado, *Appl. Catal., B* **16** (1998) 31 (https://doi.org/10.1016/S0926-3373(97)00059-3)
10. P. Liang, J. Li, X. Yang, *Microchim Acta* **152** (2005) 47 (https://doi.org/10.1007/s00604-005-0415-7)
11. D. Snigur, E. A. Azooz, O. Zhukovetska, O. Guzenko, W. Mortada, *TrAC, Trends Anal. Chem.* **164** (2023) 117113 (https://doi.org/10.1016/j.trac.2023.117113)
12. R. Halko, I. Hagarová, V. Andruch, *J. Chromatogr., A* **1701**(2023) 464053 (https://doi.org/10.1016/j.chroma.2023.464053)
13. H. S. Ferreira, M. A. Bezerra, S.L.C. Ferreira, *Microchim. Acta* **154** (2006) 163 (https://doi.org/10.1007/s00604-005-0475-8)
14. W. R. Melchert, F. R. P. Rocha, *Rev. Anal. Chem.* **35** (2016) 41 (https://doi.org/10.1515/revac-2015-0022)
15. J. Yongsheng, W. Le, L. Ruihong, W. Haohao, S. Shuhui, C. Mingzhuo, *ACS Omega* **6** (2021) 13508 (https://doi.org/10.1021/acsomega.1c01768)
16. M.N. Jones, *Int. J. Pharm.* **177** (1999) 137 (https://doi.org/10.1016/s0378-5173(98)00345-7)
17. A. Amara-Rekkab, M.A. Didi, *Desalin. Water Treat.* **281** (2022) 186 (https://doi.org/10.5004/dwt.2023.29147)
18. N. Sato, M. Morin, H. Itabashi, *Talanta* **117** (2013) 376 (https://doi.org/10.1016/j.talanta.2013.08.025)
19. A. Asfaram, M. Ghaedi, A. Goudarzi, M. Rajabi, *Dalton Trans.* **44** (2015) 14707 (https://doi.org/10.1039/C5DT01504A)
20. G. Hanrahan, K. Lu, *Crit. Rev. Anal. Chem.* **36** (2006) 141 (https://doi.org/10.1080/10408340600969478)
21. M. Boulahbal, M. A. Malouki, M. Canle, Z. Redouane-Salah, S. Devanesan, M. S. AlSalhi, M. Berkani, *Chemosphere* **306** (2022) 135516 (https://doi.org/10.1016/j.chemosphere.2022.135516)
22. H. Ucbeyiay, *Fuel Process. Technol.* **106** (2013) 1 (https://doi.org/10.1016/j.fuproc.2012.09.020)
23. G. E. B. Box, W.G. Hunter, J.S. Hunter, *Statistics for Experimenters*, 2nd ed., Wiley-Interscience, Hoboken, NJ, 1978
24. T. Mehmood, A. Ahmed, A. Asif, A. M. Sheeraz, M. A. Sandhu, *Food Chem.* **253** (2018) 179 (https://doi.org/10.1016/j.foodchem.2018.01.136)
25. S.I.S. Al-Hawary, K. Azhar, S. A. Sherzod, A.K. Kareem, K. A. Alkhuzai, R. R. M. Parra, A. H. Amini, T. Alawsi, M. Abosaooda, M. Dejaverdi, *Alex. Eng. J.* **74** (2023) 737 (https://doi.org/10.1016/j.aej.2023.05.066)
26. K. Behera, H. Meena, S. Chakraborty, B.C. Meikap, *Int. J. Min. Sci. Technol.* **28** (2018) 621 (https://doi.org/10.1016/j.ijmst.2018.04.014)

(CC) 2024 Serbian Chemical Society.

27. M. Maleki-Kakelar, A. Aghaeinejad-Meybodi, S. Sanjideh, M. J. Azarhoosh, *Environ. Proc.* **9** (2022) 7 (https://doi.org/10.1007/s40710-022-00564-0)
28. P. Mondal, A. K. Sadhukhan, A. Ganguly, P. Gupta, *3 Biotech* **11** (2021) 28 (https://doi.org/10.1007/s13205-020-02553-2)
29. N. Teslić, N. Bojanić, D. Rakić, A. Takači, Z. Zeković, A. Fišteš, M. Bodroža-Solarov, B. Pavlić, *Chem. Eng. Process.* **143** (2019) 107634 (https://doi.org/10.1016/j.cep.2019.107634)
30. B. Jiang, F. Zhang, Y. Sun, X. Zhou, J. Dong, L. Zhang, *J. Taiwan Inst. Chem. Eng.* **45** (2014) 2217 (https://doi.org/10.1016/j.jtice.2014.03.020)
31. A. Çelekli, H. Bozkurt, F. Geyik, *Bioresour. Technol.* **129** (2013) 396 (https://doi.org/10.1016/j.biortech.2012.11.085)
32. A. Smaali, M. Berkani, F. Merouane, V.T. Le, Y. Vasseghian, N. Rahim, M. Kouachi, *Chemosphere* **266** (2021) 129158 (https://doi.org/10.1016/j.chemosphere.2020.129158)
33. K. Oukebdane, R. Semmoud, M.A. Didi, *Desalin. Water Treat*. **247** (2022) 272 (https://doi.org/10.5004/dwt.2022.28039)
34. M. Berkani, M. Bouhelassa, M. K. Bouchareb, *Arab. J. Chem.* **12** (2019) 3054 (https://doi.org/10.1016/j.arabjc.2015.07.004)
35. D. Bas, I. Boya, *J. Food Eng.* **78** (2007) 836 (https://doi.org/10.1016/j.jfoodeng.2005.11.024)
36. M. Pravitha, M. R. Manikantan, V. Ajesh Kumar, S. Beegum, R. Pandiselvam, *LWT* **146** (2021) 111441 (https://doi.org/10.1016/j.lwt.2021.111441)
37. J. Han, M. Kamber, J. Pei, *Data Mining: Concepts and Techniques*, 3rd ed., Morgan Kaufmann, 2012.
38. E. Bello, T. Ogedengbe, M. Khumbulani, I. Daniyan, *Procedia CIRP* **89** (2020) 59 (https://doi.org/10.1016/j.procir.2020.05.119)
39. R. Pandiselvam, M. R. Manikantan, S. Sunoj, S. Sreejith, S. Beegum, *J. Food Process Eng.* **42** (2019) e12981 (https://doi.org/10.1111/jfpe.12981)
40. S. Youssefi, Z. Emam-Djomeh, S. M. Mousavi, *Drying Technol.* **27** (2009) 910 (https://doi.org/10.1080/07373930902988247)
41. V. Ajesh Kumar, S. Prem Prakash, M. Pravitha, H. Muzaffar, M. Shukadev, V. Prithviraj, V. Deepak Kumar, *Food Pack. Shelf Life* **31** (2022) 100778 (https://doi.org/10.1016/j.fpsl.2021.100778)
42. A. J. Sisi, A. Khataee, M. Fathinia, B. Vahid, Y. Orooji, *J. Mol. Liq.* **316** (2020) 113801 (https://doi.org/10.1016/j.molliq.2020.113801)
43. Z. Jun, C. Leland, S. Dongyi, W. Y. Zhan, *Appl. Energy* **345** (2023) 121373 (https://doi.org/10.1016/j.apenergy.2023.121373).

(CC) 2024 Serbian Chemical Society.